

Magnetic properties of two dimensional silicon carbide triangular nanoflakes-based kagome lattices

Xiaowei Li · Jian Zhou · Qian Wang ·
Puru Jena

Received: 15 January 2012 / Accepted: 12 July 2012 / Published online: 25 July 2012
© Springer Science+Business Media B.V. 2012

Abstract Two-dimensional (2D) magnetic kagome lattices are constructed using silicon carbide triangular nanoflakes (SiC-TNFs). Two types of structures with alternating Si and C atoms are studied: the first one is constructed using the C-edged SiC-TNFs as the building blocks and C atoms as the linkers of kagome sites ($\text{TNF}_N\text{-C-TNF}_N$) while the second one is composed of the Si-edged SiC-TNFs with Si atoms as linkers ($\text{TNF}_N\text{-Si-TNF}_N$). Using density functional theory-based calculations, we show that the fully relaxed $\text{TNF}_N\text{-C-TNF}_N$ retains the morphology of regular kagome lattice and is ferromagnetic. On the other hand, the $\text{TNF}_N\text{-Si-TNF}_N$ structure is deformed and antiferromagnetic. However, the ground state of $\text{TNF}_N\text{-Si-TNF}_N$ structure can be transformed from the antiferromagnetic to ferromagnetic state by applying tensile strain. Monte Carlo simulations indicate that

the SiC-TNFs-based kagome lattices can be ferromagnetic at room temperature.

Keywords Silicon carbide triangular nanoflake · Kagome lattice · Magnetic coupling · Tensile strain · First principle calculation · Monte Carlo simulation

Introduction

Carbon-based magnetic materials where magnetism originates from C $2p$ orbitals are potential candidates for spintronic devices due to weak spin-orbit coupling and hyperfine interactions (Yazyev 2010). Zigzag-edged graphene nanoribbons (GNRs) and graphene triangular nanoflakes (G-TNFs) have recently attracted considerable attention as building blocks of novel magnetic materials. Although the opposite two edges of a GNR couple antiferromagnetically (Lee et al. 2005; Gunlyckea et al. 2007; Son et al. 2006), they can be made to couple ferromagnetically (FM) by charge doping (Sawada et al. 2009) or by supporting them on magnetic substrates (Sawada et al. 2010). The three zigzag edges of a G-TNF couple ferromagnetically (Şahin et al. 2010; Wang et al. 2008; Ezawa 2009; Rocha et al. 2010; Akola et al. 2008; Philpott et al. 2010; Potasz et al. 2011; Fernández-Rossier et al. 2007), and have a size-dependent magnetic moment of $(N - 1) \mu_B$, where N is the number of hexagons along one edge of the G-TNF. While much emphasis has

This article is part of the topical collection on nanomaterials in energy, health and environment

X. Li · Q. Wang (✉)
Center for Applied Physics and Technology, College of
Engineering, Peking University, Beijing 100871, China
e-mail: qianwang2@pku.edu.cn

J. Zhou
Department of Materials Science and Engineering, Peking
University, Beijing 100871, China

Q. Wang · P. Jena
Department of Physics, Virginia Commonwealth
University, Richmond, VA 23284, USA

been placed on studying C-based magnetic materials, not much work has been carried out on exploring magnetism of SiC-based materials. We note that bulk SiC possesses unique physical properties, such as high hardness, high thermal conductivity, and superior radiation resistance, which are ideal for applications in electronic and optical devices. Therefore, it is highly desirable to see if low-dimensional SiC materials can exhibit novel magnetic behavior and if their properties can be further improved over C-based materials. This is particularly important since various kinds of low-dimensional SiC structures, such as one dimensional (1D) SiC nanorods (Dai et al. 1995; Wong et al. 1997), nanowires (Zhou et al. 2006; Yang et al. 2007), and nanotubes (Sun et al. 2002; Pham-Huu et al. 2001) have been successfully synthesized. Theoretical study on single-walled SiC nanotubes has shown that the energetically favorable structure is one where Si and C atoms alternatively occupy hexagonal sites of the nanotubes (Mavrandonakis et al. 2003; Menon et al. 2004; Alam et al. 2007, 2008). Here Si and C atoms are all sp^2 hybridized, similar to C atoms in single-walled carbon nanotubes. Therefore, we could expect that zigzag-edged SiC-TNFs with alternating Si and C atoms would have similar magnetic behaviors as those of G-TNFs. We demonstrated that the G-TNFs can indeed be used as magnetic building blocks to assemble the 2D porous carbon-based FM materials (Zhou et al. 2011). The questions we address are: what is the magnetic behavior like of the SiC-TNFs? Can one construct a 2D FM periodic structure using SiC-TNFs as the building blocks? How can its magnetic properties be controlled?

We have used the kagome lattice to construct SiC-TNFs-based materials. A kagome lattice, a mathematical model, composed of interlaced triangles in a 2D pattern, is usually used to study the frustrated magnetism (Syôzi 1951) and design materials with high Curie–Weiss temperature. For example, Ramirez et al. (1990) studied $\text{SrCr}_8\text{Ga}_4\text{O}_{19}$ where Cr ions form a kagome lattice with high Curie–Weiss temperature of 515 K. Recently, Schweika et al. (2007) synthesized the layered kagome materials consisting of $\text{Y}_{0.5}\text{Ca}_{0.5}\text{BaCo}_4\text{O}_7$ which exhibits even higher Curie–Weiss temperature of 2,200 K. In the present study, the zigzag-edged SiC-TNFs were used as the building blocks of kagome lattices. Using spin-polarized density functional theory together with Monte Carlo simulations, we show that the constructed 2D

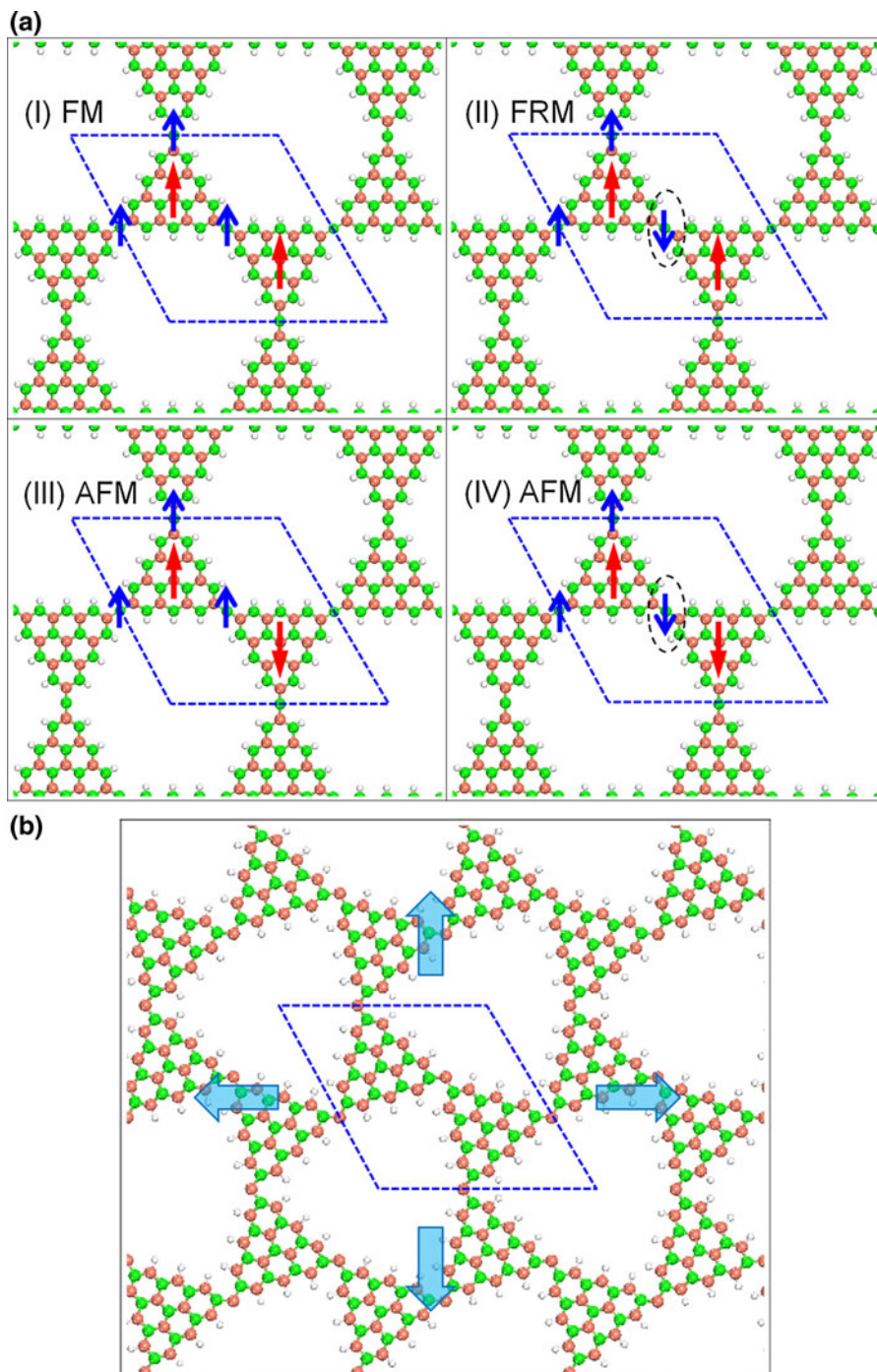
periodic kagome lattices are FM with Curie point close to room temperature.

Theoretical procedure

Two types of the 2D periodic structures are generated. The first one is constructed by inserting the C-edged SiC-TNFs into the nearest triangles of kagome lattice and C atoms at kagome sites, while the second one is constructed using the Si-edged SiC-TNFs as building blocks with Si atoms as linkers (see Fig. 1). The unit cell of both the structures contains two of the SiC-TNFs and three linking atoms (C or Si). The generated 2D periodic structures are labeled as $\text{TNF}_N\text{-C-TNF}_N$ and $\text{TNF}_N\text{-Si-TNF}_N$, respectively, where N is the number of hexagons along one edge of the SiC-TNF $_N$, representing size of the TNFs.

Spin-polarized density functional theory implemented in the Vienna ab initio Simulation Package (VASP code) (Kresse et al. 1996) were used to perform the calculations. A vacuum space of 12 Å was used in the perpendicular direction of the 2D sheet. The exchange–correlation potential based on the generalized gradient approximation (GGA) (Perdew et al. 1996) as prescribed by Perdew–Burke–Ernzerhof (PBE) was employed. Monkhorst–Pack special k -point mesh of $7 \times 7 \times 1$ was used to represent the Brillouin zone for the structures composed of the SiC-TNF $_N$ s with $N = 2, 3$. The energy cutoff and the convergence criteria of energy and force were set to be 400 eV, 0.01 meV, and 0.001 eV/Å, respectively. All atoms were fully relaxed by conjugate-gradient algorithm. In order to determine the preferred magnetic coupling between the SiC-TNF $_N$ s, four kinds of spin coupling configurations labeled as I, II, III, and IV, as shown in Fig. 1a, were considered. The energy difference ΔE between the FM state and the ferrimagnetic/antiferromagnetic (FRM/AFM) state was defined as $\Delta E = E_{\text{FRM/AFM}} - E_{\text{FM}}$. Positive value of ΔE means the FM state lies lower in energy than the FRM/AFM state. Monte Carlo simulations were further carried out for a (10×10) supercell system to study the magnetic behavior of this periodic structure at finite temperatures. The Ising model Hamiltonian, $H = -\sum_{\langle i,j \rangle} J_{ij}S_iS_j$, is used where i and j represent two nearest-neighbor magnetic sites, namely the linking atom and the TNF $_N$, and J is the exchange parameter. 1×10^5 steps were used to

Fig. 1 Geometries of the 2D periodic structures of **a** $\text{TNF}_3\text{-C-TNF}_3$ and **b** $\text{TNF}_3\text{-Si-TNF}_3$. Green, orange, and white spheres represent C, Si, and H atoms, respectively. The blue dashed lines indicate a unit cell. Blue and red arrows in (a) denote the spin directions of kagome sites and the TNFs. The directions of applied tensile strain on the $\text{TNF}_3\text{-Si-TNF}_3$ are given by large blue arrows in (b). (Color figure online)



simulate the data. The accuracy of our simulation procedure has been established in our previous work on the 2D FM carbon-based structures assembled using odd-numbered C-chains as spin-containing components and 1,3,5-benzenetriyl units as ferromagnetic coupling units (Li et al. 2011).

Results and discussion

We first examined the magnetic configuration for a single flake. The FM states of the C-edged and Si-edged TNF_3 s are 0.16 and 0.21 eV lower in energy than the corresponding paramagnetic (PM) states,

respectively. Therefore, we conclude that the ground state of a single flake is FM. The fully relaxed 2D structures of $\text{TNF}_N\text{-C-TNF}_N$ and $\text{TNF}_N\text{-Si-TNF}_N$ with $N = 3$ are quite different, as shown in Fig. 1a,b, respectively. The first one is an undistorted kagome lattice composed of the C-edged SiC-TNF_3 with C atoms occupying the kagome sites, whereas the second one undergoes a large deformation upon geometry relaxation. We use two parameters to describe the geometric structure of the systems: θ (the angle among the linking atom and its nearest two atoms) and L_0 (lattice parameter of the unit cell). Due to the geometric deformation, the $\text{TNF}_3\text{-Si-TNF}_3$ has smaller θ (112°) and L_0 (23.51 \AA), as compared to the $\text{TNF}_3\text{-C-TNF}_3$ structure ($\theta = 180^\circ$, and $L_0 = 24.72 \text{ \AA}$). The calculated results including the geometric parameters (θ and L_0), the energy differences (ΔE) between the FM and FRM/AFM states, and the magnetic moments (M) of one unit cell of the $\text{TNF}_3\text{-C-TNF}_3$ and $\text{TNF}_3\text{-Si-TNF}_3$ are tabulated in Table 1.

For the 2D periodic $\text{TNF}_3\text{-C-TNF}_3$ structure, we found that the FM coupling configuration (I) is the ground state with the FM state lying $0.32 \text{ eV/unit cell}$ lower in energy than the AFM configuration (IV). The AFM coupling configuration (III) lies $0.33 \text{ eV/unit cell}$ higher in energy than the FM configuration, which is nearly energetically degenerate with the AFM configuration (IV). However, the FRM coupling configuration (II) lies a smaller value of $0.22 \text{ eV/unit cell}$ higher in energy than the FM configuration. On the other hand, for the $\text{TNF}_3\text{-Si-TNF}_3$, the AFM coupling configuration (IV) is found to be the ground

state with the FM configuration (I) being higher in energy by $0.01 \text{ eV/unit cell}$. The small energy difference implies a weak magnetic interaction between the SiC-TNF_3 s. The FRM (II) and AFM (III) configurations were energetically degenerate with the FM (I) and AFM (IV) ones, respectively, indicating that the spin direction of Si atoms has no effect on the magnetic coupling between the TNFs. The total magnetic moment of the $\text{TNF}_3\text{-C-TNF}_3$ is calculated to be $10.00 \mu_B/\text{unit cell}$. This is because each C-edged SiC-TNF_3 contributes $2.0 \mu_B$ and each linking C atom carries a moment of $2.0 \mu_B$. Note that a unit cell of the 2D $\text{TGF}_3\text{-C-TGF}_3$ structure contains two C-edged SiC-TNF_3 and three C linking atoms. The total magnetic moment for the $\text{TGF}_3\text{-Si-TGF}_3$ is found to be $0.00 \mu_B/\text{unit cell}$ due to its AFM coupling feature.

To study the size dependence, we further considered the $\text{TNF}_N\text{-C-TNF}_N$ and $\text{TNF}_N\text{-Si-TNF}_N$ structures with $N = 2$. Following the same procedure as described above, we found that the optimized structures have the same geometrical feature as the bigger ones, namely a regular kagome lattice for the $\text{TNF}_2\text{-C-TNF}_2$ and a deformed kagome lattice for the $\text{TNF}_2\text{-Si-TNF}_2$. For the $\text{TNF}_2\text{-C-TNF}_2$ structure, the FM coupling configuration (I) is also found to be the ground state, which is 0.16 , 0.28 , and $0.31 \text{ eV/unit cell}$ lower in energy than the FRM (II), AFM (III), and AFM (IV) configurations, respectively. The magnetic moment was calculated to be $8 \mu_B/\text{unit cell}$. Once again, we see that a FM kagome lattice can be assembled using the C-edged SiC-TNF_2 s as building blocks and C atoms as linkers. For the $\text{TNF}_2\text{-Si-TNF}_2$ structure, however, the AFM state is again found to be lower in energy than any other spin coupling configurations. We note that the energy difference of $\Delta E^{(\text{III})}$ (0.28 eV) is smaller than that of $\Delta E^{(\text{IV})}$ (0.31 eV) indicating that they are not degenerate any more, and the FRM state (II) also has a smallest energy difference of $\Delta E^{(\text{II})}$ (0.16 eV) when $N = 2$. For the deformed structure of $\text{TNF}_2\text{-Si-TNF}_2$, the AFM coupling configurations (III and IV), see Fig. 1a for reference, are always energetically degenerated, indicating that Si atom does not play any role in mediating the magnetic coupling between the SiC-TNF_2 s.

In order to view the magnetic moment distribution in real space, we plotted the iso-surfaces of spin density for the ground states of $\text{TNF}_3\text{-C-TNF}_3$ and $\text{TNF}_3\text{-Si-TNF}_3$ structures in Fig. 2a,b, respectively. They show that for both of them, the spin majority is

Table 1 Geometric parameters θ (in degree) and L_0 (in \AA), the energy difference ΔE (in eV/unit cell) between the FM and FRM/AFM states

Structures	$\text{TNF}_3\text{-C-TNF}_3$	$\text{TNF}_3\text{-Si-TNF}_3$
θ	180°	112°
L_0	24.72	23.51
$\Delta E^{(\text{II})}$	0.22	0.00
$\Delta E^{(\text{III})}$	0.33	-0.01
$\Delta E^{(\text{IV})}$	0.32	-0.01
M	10.00	0.00

II, III, and IV correspond to the FRM (II), AFM (III), and AFM (IV) spin coupling configurations, as shown in Fig. 1a, respectively, and magnetic moment M (in $\mu_B/\text{unit cell}$) for the 2D $\text{TNF}_3\text{-C-TNF}_3$ and $\text{TNF}_3\text{-Si-TNF}_3$ structures

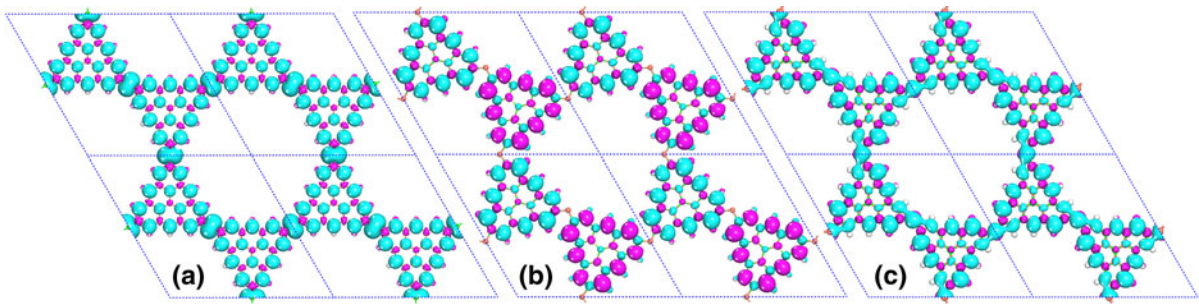


Fig. 2 Spin density iso-surfaces at the value of $0.005 \mu_B \text{ \AA}^{-3}$. **a** $\text{TNF}_3\text{-C-TNF}_3$. **b** $\text{TNF}_3\text{-Si-TNF}_3$. **c** $\text{TNF}_3\text{-Si-TNF}_3$ with a tensile strain of 11 %

localized on the sublattice A sites of the TNFs, while the minority spin is on the sublattice B sites. The magnetic moment mainly comes from the $2p$ orbitals of C or $3p$ orbitals of Si atoms at the A sites. The most notable difference between these two kinds of structures is that the C atoms at kagome sites have a large net spin and make a large contribution ($2.0 \mu_B$) to the magnetic moment, while the Si atoms at kagome sites have zero contribution to the magnetic moment, resulting in a weak interaction and AFM coupling between the SiC-TNFs. It is interesting to see that although C and Si belong to the same group in the periodical table, they have very different effects on the magnetic coupling between the SiC-TNFs. The band structures of $\text{TNF}_3\text{-C-TNF}_3$ and $\text{TNF}_3\text{-Si-TNF}_3$ are plotted in Fig. 3, which show that both of the two structures are semiconducting with small gaps.

We then studied the effect of structural deformation on magnetism by applying tensile strain on the deformed $\text{TNF}_N\text{-Si-TNF}_N$ structure. The purpose is to see if one can tune the magnetic coupling between the TNFs (see Fig. 1b). Here, tensile strain is defined as $\text{TS} = (L - L_0)/L_0 \times 100 \%$, and L and L_0 are the lattice parameters of the strained and unstrained $\text{TNF}_N\text{-Si-TNF}_N$ structures, respectively. Taking $N = 3$ as an example, the change in the energy difference with increasing tensile strain is plotted in Fig. 4. It shows that the energy difference $\Delta E (E_{\text{AFM}} - E_{\text{FM}})$ increases with the tensile strain, and the FM coupling configuration becomes energetically more favorable when the applied tensile strain is larger than 2 %. When the tensile strain is further increased to larger than 7 %, the energy difference ΔE increases nonlinearly, and the FM coupling configuration becomes more stable. The corresponding change of the spin density distribution is plotted in Fig. 2c, which shows that the spin

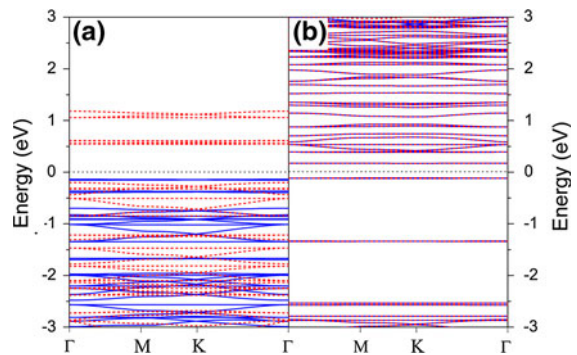


Fig. 3 Band structures of **a** $\text{TNF}_3\text{-C-TNF}_3$ and **b** $\text{TNF}_3\text{-Si-TNF}_3$. The black dotted lines represent Fermi surfaces. Blue and red lines represent spin up and spin down, respectively. (Color figure online)

density of Si atoms at kagome sites makes a significant contribution to the magnetic moment, and the Si atoms couple ferromagnetically with their neighboring TNFs, resulting in a FM-strained $\text{TNF}_3\text{-Si-TNF}_3$ structure.

Finally, we investigated the magnetic behavior of the 2D FM $\text{TNF}_N\text{-C-TNF}_N$ structure at finite temperatures by performing Monte Carlo simulations. We considered the system composed of the C-edged SiC-TNF₃s, as an example. Using Ising model including the nearest and the next-nearest-neighbor interactions, the total energies of magnetic configurations (I) ~ (IV) can be expressed as following:

$$E^{(I)} = 6J_{\text{CT}}S_{\text{C}}S_{\text{T}} + 6J_{\text{CC}}S_{\text{C}}S_{\text{C}} + 3J_{\text{TT}}S_{\text{T}}S_{\text{T}}$$

$$E^{(II)} = 2J_{\text{CT}}S_{\text{C}}S_{\text{T}} - 2J_{\text{CC}}S_{\text{C}}S_{\text{C}} + 3J_{\text{TT}}S_{\text{T}}S_{\text{T}}$$

$$E^{(III)} = 0J_{\text{CT}}S_{\text{C}}S_{\text{T}} + 6J_{\text{CC}}S_{\text{C}}S_{\text{C}} - 3J_{\text{TT}}S_{\text{T}}S_{\text{T}}$$

$$E^{(IV)} = 0J_{\text{CT}}S_{\text{C}}S_{\text{T}} - 2J_{\text{CC}}S_{\text{C}}S_{\text{C}} - 3J_{\text{TT}}S_{\text{T}}S_{\text{T}}$$

The J and S are exchange parameter and magnetic moment, respectively. The subscript C and T denote

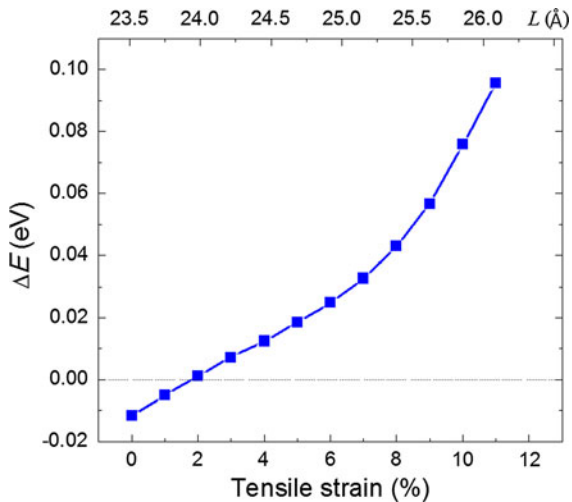


Fig. 4 Variation of energy differences ΔE per unit cell of the deformed $\text{TNF}_3\text{-Si-TNF}_3$ structure as a function of tensile strain (bottom) and lattice parameter L (top)

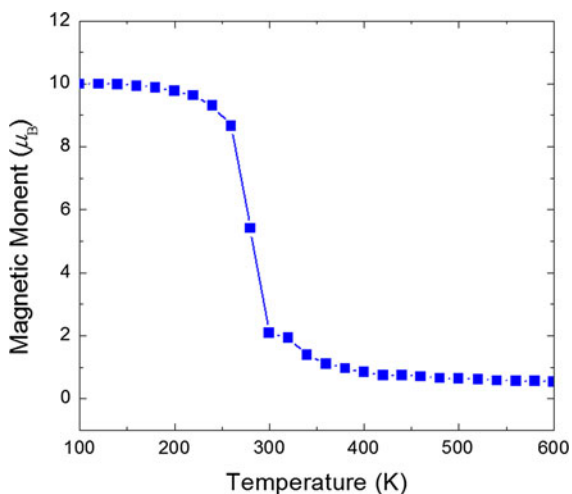


Fig. 5 Changes in the magnetic moment per unit cell of the 2D $\text{TNF}_3\text{-C-TNF}_3$ structure as a function of temperature

the linking C atom and the SiC-TNF_3 flake, respectively. We can deduce the exchange parameters J_{CT} , J_{CC} , and J_{TT} by our calculated results $\Delta E^{(\text{II})}$, $\Delta E^{(\text{III})}$, and $\Delta E^{(\text{IV})}$, respectively. We find that $J_{\text{CT}} = -13.75$ meV, $J_{\text{CC}} = 0$ meV, and $J_{\text{TT}} = 0.41$ meV. It is obvious that the next-nearest-neighbor interaction parameters J_{CC} and J_{TT} are much less than the J_{CT} . Therefore, only the nearest-neighbor interactions are considered in our Monte Carlo simulation, which is sufficient to study the main physical behaviors of the system. The variation of magnetic moment per unit cell with respect to temperature is plotted in Fig. 5. We

see that the magnetic moment remains nearly at $10 \mu_{\text{B}}$ until 200 K, and then it sharply decreases as temperature increases further. The sudden drop of magnetic moment occurs at around 290 K which corresponds to the Curie temperature. It is larger than those of dilute magnetic semiconductors such as (Ga, Mn) N (Sato et al. 2010), suggesting that this system could have applications at near room temperature.

Conclusion

In conclusion, we studied the magnetic properties of kagome lattices composed of the C- and Si-edged SiC-TNF_3 where C and Si atoms, respectively, serve as linkers. The calculated results show that the assembled 2D $\text{TNF}_N\text{-C-TNF}_N$ structure is FM, which is different from the $\text{TNF}_N\text{-Si-TNF}_N$ structure where the AFM state is energetically more stable. However, the AFM ground state of $\text{TNF}_N\text{-Si-TNF}_N$ structure can be transformed to the FM state when the tensile strain is applied. Monte Carlo simulations indicate that the predicted ferromagnetism in the SiC-TNF_3 -based kagome lattices can be detected at room temperature. We hope that this work will stimulate experimental investigation and that SiC-TNF_3 -based FM kagome lattices can have potential applications in the next generation spintronic devices.

Acknowledgments This work is supported by Grants from the National Natural Science Foundation of China (Grant No. NSFC-11174014), the National Grand Fundamental Research 973 Program of China (Grant No. 2012CB921404), and from the US Department of Energy. This research used resources of the National Energy Research Scientific Computing Center, which is supported by the Office of Science of the U.S. Department of Energy under Contract No. DE-AC02-05CH11231. Xiaowei Li would like to acknowledge the support from China Postdoctoral Science Foundation (Grant No. 2012M510246).

References

- Akola J, Heiskanen HP, Manninen M (2008) Edge-dependent selection rules in magic triangular graphene flakes. *Phys Rev B* 77:193410
- Alam KM, Ray AK (2007) A hybrid density functional study of zigzag SiC nanotubes. *Nanotechnology* 18:495706
- Alam KM, Ray AK (2008) Hybrid density functional study of armchair SiC nanotubes. *Phys Rev B* 77:035436
- Dai H, Wong EW, Lu YZ, Fan SS, Lieber CM (1995) Synthesis and characterization of carbide nanorods. *Nature* 375:769–772

- Ezawa M (2009) Quasiphase transition and many-spin kondo effects in a graphene nanodisk. *Phys Rev B* 79:241407(R)
- Fernández-Rossier J, Palacios JJ (2007) Magnetism in graphene nanoislands. *Phys Rev Lett* 99:177204
- Gunlycke D, Li J, Mintmire JW, White CT (2007) Altering low-bias transport in zigzag-edge graphene nanostrips with edge chemistry. *Appl Phys Lett* 91:112108
- Kresse G, Furthmüller J (1996) Efficient iterative schemes for *ab initio* total-energy calculations using a plane-wave basis set. *Phys Rev B* 54:11169
- Lee H, Son Y-W, Park N, Han S, Yu J (2005) Magnetic ordering at the edges of graphitic fragments: magnetic tail interactions between the edge-localized states. *Phys Rev B* 72:174431
- Li XW, Wang Q, Jena P (2011) Ferromagnetism in two-dimensional carbon chains linked by 1,3,5-benzenetriyl units. *J Phys Chem C* 115:19621
- Mavrandonakis A, Froudakis GE, Schnell M, Mühlhäuser M (2003) From pure carbon to silicon-carbon nanotubes: an *ab initio* study. *Nano Lett* 3:1481–1484
- Menon M, Richter E, Mavrandonakis A, Froudakis G, Andriotis AN (2004) Structure and stability of SiC nanotubes. *Phys Rev B* 69:115322
- Perdew JP, Burke K, Ernzerhof M (1996) Generalized gradient approximation made simple. *Phys Rev Lett* 77:3865
- Pham-Huu C, Keller N, Ehret G, Ledoux MJ (2001) The first preparation of silicon carbide nanotubes by shape memory synthesis and their catalytic potential. *J Catal* 200:400–410
- Philpott MR, Vukovic S, Kawazoe Y, Lester WA (2010) Edge versus interior in the chemical bonding and magnetism of zigzag edged triangular graphene molecules. *J Chem Phys* 133:044708
- Potasz P, Güçlü AD, Voznyy O, Folk JA, Hawrylak P (2011) Electronic and magnetic properties of triangular graphene quantum rings. *Phys Rev B* 83:174441
- Ramírez AP, Espinosa GP, Cooper AS (1990) Strong frustration and dilution-enhanced order in a quasi-2D spin glass. *Phys Rev Lett* 64:2070
- Rocha AR, Martins TB, Fazzio A, da Silva AJR (2010) Magnetism and perfect spin filtering effect in graphene nanoflakes. *Nanotechnology* 21:345202
- Şahin H, Senger RT, Ciraci S (2010) Spintronic properties of zigzag-edged triangular graphene flakes. *J Appl Phys* 108:074301
- Sato K, Bergqvist L, Kudrnovský J, Dederichs PH, Eriksson O, Turek I, Sanyal B, Bouzerar G, Katayama-Yoshida H, Dinh VA, Fukushima T, Kizaki H, Zeller R (2010) First-principles theory of dilute magnetic semiconductors. *Rev Mod Phys* 82:1633–1690
- Sawada K, Ishii F, Saito M, Okada S, Kawai T (2009) Phase control of graphene nanoribbon by carrier doping: appearance of noncollinear magnetism. *Nano Lett* 9:269–272
- Sawada K, Ishii F, Saito M (2010) Magnetism in graphene nanoribbons on Ni(111): first-principles density functional study. *Phys Rev B* 82:245426
- Schweika W, Valldor M, Lemmens P (2007) Approaching the ground state of the kagomé antiferromagnet. *Phys Rev Lett* 98:067201
- Son Y-W, Cohen ML, Louie SG (2006) Energy gaps in graphene nanoribbons. *Phys Rev Lett* 97:216803
- Sun X-H, Li CP, Wong WK, Wong NB, Lee CS, Lee ST, Teo BK (2002) Formation of silicon carbide nanotubes and nanowires via reaction of Silicon (from disproportionation of silicon monoxide) with carbon nanotubes. *J Am Chem Soc* 124:14464–14471
- Syózi I (1951) Statistics of kagomé lattice. *Prog Theor Phys* 6:306
- Wang WL, Meng S, Kaxiras E (2008) Graphene nanoflakes with large spin. *Nano Lett* 8:241–245
- Wong EW, Sheenhan PE, Lieber CM (1997) Nanobeam mechanics: elasticity, strength, and toughness of nanorods and nanotubes. *Science* 277:1971–1975
- Yang GY, Wu RB, Chen JJ, Pan Y, Zhai R, Wu LL, Lin J (2007) Growth of SiC nanowires/nanorods using a Fe–Si solution method. *Nanotechnology* 18:155601
- Yazyev OV (2010) Emergence of magnetism in graphene materials and nanostructures. *Rep Prog Phys* 73:056501
- Zhou WM, Liu X, Zhang YF (2006) Simple approach to β -SiC nanowires: synthesis, optical, and electrical properties. *Appl Phys Lett* 89:223124
- Zhou J, Wang Q, Sun Q, Jena P (2011) Intrinsic ferromagnetism in two-dimensional carbon structures: triangular graphene nanoflakes linked by carbon chains. *Phys Rev B* 84:081402(R)